

Co-culture Based Blood-brain Barrier In Vitro Model, a Tissue Engineering Approach using Immortalized Cell Lines for Drug Transport Study

Zhiqi Zhang · Anthony J. McGoron · Eric T. Crumpler ·
Chen-Zhong Li

Received: 6 May 2010 / Accepted: 4 July 2010 /
Published online: 24 July 2010
© Springer Science+Business Media, LLC 2010

Abstract This study evaluated the feasibility of using commercially available immortalized cell lines in building an in vitro blood-brain barrier (BBB) co-culture model for preliminary drug development studies. Astrocytes-derived acellular extracellular matrix (aECM) was introduced in the co-culture model to provide a novel biomimetic basement membrane for the endothelial cells to form tight junctions. Trans-Endothelial Electrical Resistance (TEER) and solute mass transport studies quantitatively evaluated the tight junction formation. Immuno-fluorescence microscopy and Western blot analysis qualitatively verified the expression of occludin, one of the tight junction proteins on the samples. Experimental data from a total of 13 experiments conclusively showed that the novel BBB in vitro co-culture model with aECM (CO+aECM) is promising in terms of establishing tight junction formation represented by TEER values, transport profiles, and tight junction protein expression when compared with traditional co-culture (CO) model setup or the endothelial cells cultured alone (EC). In vitro colorimetric sulforhodamine B (SRB) assay also revealed that the “CO+aECM” samples resulted in less cell loss on the basal sides of the insert membranes than traditional co-culture models. Our novel approach using immortalized cell lines with the addition of aECM was proven to be a feasible and repeatable alternative to the traditional BBB in vitro modeling.

Keywords Blood-brain barrier · Co-culture · In vitro · Transport · Drug delivery · Membrane impedance · Western blot · Tight junction · Occludin

Introduction

According to the Brain Tumor Society, over 200,000 people are diagnosed with a primary or metastatic brain tumor in the US each year. However, the current available drug delivery methods are usually risky, highly invasive, can lead to irreversible side effects or allow very

Z. Zhang · A. J. McGoron · E. T. Crumpler · C.-Z. Li (✉)
Department of Biomedical Engineering, Florida International University, 10555 W. Flagler St, Miami,
FL 33174, USA
e-mail: licz@fiu.edu

limited distribution of drug within the brain tissue—for example, injecting hyper osmotic sugar solutions (Mannitol) into a brain artery, inserting catheters to pump drugs into the brain and implanting drug eluting wafers after surgical tumor removal [1]. The biggest challenge in brain drug delivery research is to overcome the brain's effective protective mechanism collectively known as the blood-brain barrier (BBB) [2–5]. The use of BBB in vitro culture assays in early safety assessment of drugs is still growing [5].

As a complex environment, the BBB is composed of brain capillary endothelial cells, astrocytes, and pericytes [6, 7]. Transcellular flux is limited by very few endocytotic vesicles present on the BBB, and paracellular flux is severely restricted by tight junctions between brain microvascular endothelial cells. The tight junctions in the BBB are characterized as the apical junctional complex between brain microvascular endothelial cells [8, 9]. Several molecular components are unique to the tight junction, such as occludin, claudins, zonula occludens, and junctional adhesion molecules [8, 10]. Among these constituents of tight junction strands, occludin was the first to be identified [8]. Several studies showed that occludin may be involved in signal transduction and thus an important component of the BBB [10–15].

Astrocytes are a type of glial cell responsible for secreting extracellular matrix (ECM) molecules that exist in the cerebral microenvironment [16]. It is believed that astrocytes regulate the induction of the BBB in tight junction formation and upregulate the expression of transport systems [8, 17]. They make contact with the brain vasculature through end feet which ensheath the ECs onto which they form rosette-like structures [9]. In addition, astrocytes are considered the major producer of adhesion molecules in the central nervous system (CNS). Evidence has also shown that integrin matrix adhesion receptors secreted by brain astrocytes and endothelial cells are important in maintaining BBB permeability [18, 19]. Because of the importance of astrocytes in the formation and maintenance of the BBB, astrocytes-derived acellular extracellular matrix (aECM) as the biomimetic basement membrane for endothelial cells was considered a vital yet novel contributor in our in vitro study. While it's considered to be important in the integral BBB structure, the pericyte's roll in the BBB formation remains unclear [6].

Co-culture systems with endothelial cells and astrocytes are still, by far, the most widely used in vitro BBB modeling methods for drug delivery studies [20]. Different cell models such as bovine brain endothelial cells, human primary brain endothelial cells, MDCK cells lines, and caco-2 cell lines have been used in the existing in vitro BBB models [21]. However, most of the current successful BBB in vitro models are based on primary cell cultures. The reason for choosing primary cell cultures is mainly because of their relatively high correlations with in vivo models in terms of high TEER values and tight junction proteins expression. However, the seemingly high correlation inevitably diminishes within several passages of initial cultures [22, 23]. Besides, the availability of the primary cells can be limited for primary cultures because of the accessibility of the animals. Pathogens and donor-to-donor variability account for other major drawbacks of primary cell cultures [22, 24]. The repeatability and consistency of the in vitro models are thus unappealing. With this in mind, commercially available immortalized cell lines can be considered as an alternative. Our study utilized immortalized rat astrocytes and mouse brain endothelial cells as the building blocks of the in vitro BBB modeling system. Several advantages of using commercially available immortalized cell lines are: (1) reliability: cells can be purchased from trusted well-established sources; (2) consistency: the variance between different batches of experiments can be minimized since the cell source is controlled and consistent; (3) longevity: immortalized cell lines are specially treated by a transfection process so that the important cell features do not disappear over time [25, 26]; (4) accessibility: cells are

available to be purchased at any time, waiting time for the cell source can be confidently diminished; (5) efficiency: preparation time and cost are reduced because the cells can be immediately used upon purchase. To our best knowledge, no group has reported results from *in vitro* BBB models with aECM using either commercially available immortalized or lab-derived primary cell lines.

Materials and Methods

Materials and Reagents

Mouse endothelial cells from yolk sac (CRL-2583) and rat astrocyte from 1-day-old rats (CRL-2006) were purchased from American Type Culture Collection (ATCC; Manassas, VA). Phenol red-free Dulbecco's Modified Eagle's Medium (DMEM), 0.25% Trypsin/EDTA, Penicillin–Streptomycin–Glutamine, Dulbecco's phosphate-buffered saline (PBS), and distilled water were purchased from Invitrogen (Carlsbad, CA). Canted neck-vented cap flasks, Corning Costar® 24-well plates, Corning Costar® Collagen I and III-coated (COL) Transwell inserts for 24-well plates (more information of the membrane material to be found on the manufacturer's selection guide), 0.4 µm and bovine serum albumin (BSA) were purchased from Fisher Scientific (Pittsburgh, PA). Fetal bovine serum was purchased from Hyclone (Logan, UT). Stericup 0.22-µm filter units were purchased from Millipore (Billerica, MA). Caffeine, Doxorubicin, Calcein, SRB cytotoxicity assay kit (including 0.4% SRB solution, trichloroacetic acid (TCA)), 10 mM unbuffered Trizma base solution 99.5% glacial acetic acid, Silica Spectrophotometer cuvettes, and cuvette washer and drier were purchased from Sigma–Aldrich (St. Louis, MO; Manassas, VA).

Astrocytic aECM

The confluent astrocytes cell layer was found to “come off the culture surface in a sheet” and reported to be difficult to dissociate in previous studies [27]. The phenomenon was consistent with the observation in our experiment. At the end of the 10-day culturing period, a layer of confluent astrocytes was formed. This cell layer was resilient and could even endure normal trypsinization procedure without breaking up. This feature was utilized in our research to produce the aECM.

Briefly, rat astrocytes were seeded at the density of 2×10^4 cells/well on a 12-well plate. The culture media (DMEM) supplemented with 10% FBS and 1% Penicillin/Streptomycin was changed daily in order to achieve the best proliferation of the cell layers. The cells were kept growing for a consecutive 10-day period until full confluency was reached. On the last day, the media was removed and the confluent cell layers were rinsed with cold PBS. The cells were then incubated with 0.5 M urea for 10 min to lyse the cells at room temperature. After the treatment, the cells were decellularized and ready to be used as aECM in the *in vitro* model. The resulting aECM was rinsed with PBS carefully ten times. The aECM could then be kept soaked in PBS and stored at 4 °C for up to 2 weeks.

In Vitro BBB Models

The *in vitro* model of interest was a co-cultured model which consisted of endothelial cells and astrocytes grown on either side of the COL Transwell inserts, with the addition of aECM right before ECs were seeded (CO+aECM). Briefly, 5,000 astrocytes were seeded

on the basal side of the inserts at the beginning of the culture period. After 3 days of incubation, the inserts were inverted to their original orientation and returned to the 24-well plates. A piece of aECM, produced as previously described, was placed into each individual insert cup and then 10,000 endothelial cells were seeded on top of the aECM. All the plates were incubated at 37 °C in an atmosphere with 5% CO₂. The control groups were: endothelial cells plated alone on the upper sides of the inserts (EC), and the traditional co-culture (CO) setup where endothelial cells were seeded on the upper sides of the inserts and astrocytes grown on the basal sides of the inserts. Figure 1 shows the schematic of the “CO+aECM” sample.

TEER Measurements

The cells took around 24 h to recover from dissociation trauma before normal proliferation occurred. Thus all the cultured samples were left intact for the first day after the endothelial cells were seeded. TEER values for all the setups were measured by EVOM[®] epithelial voltohmmeter with EndOhm tissue resistance measurement chamber specially designed for tissue culture inserts (World Precision Instruments, Sarasota, FL). The measurements were taken daily starting from 2 days after the endothelial cells were seeded. The results were expressed in ohms square centimeter, which were calculated by multiplying the meter readings by the effective surface area of the filter membrane (0.33 cm²). The TEER value for a blank insert was measured everyday alongside the sample measurements. The final TEER values displayed in the “Results” were measured values minus blank TEER values.

Transport Studies on In Vitro Models

At the end of the culturing period, transport across selected sample membranes was studied using calcein (Sigma), caffeine (Sigma), and Doxorubicin (Sigma) solutions. Because of the on-campus facility restraints, test results were measured by an optical spectrometer (Cary 100 UV-Vis spectrophotometer, Varian) with UV absorbance scans instead of the more popular radio activity scintillation counting. Initially, all the compounds were prepared by dissolving original powder with phenol red-free DMEM (Gibco) to reach the stock concentration of 50 µg/ml (which is the optimal concentration for the spectrophotometer’s working range).

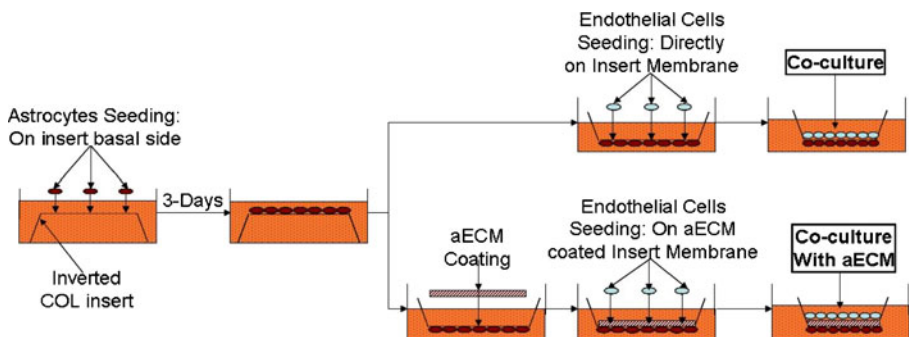


Fig. 1 Schematic of BBB in vitro co-cultured setup. Displayed are two setups which both start from the astrocyte seeding on the basal sides of the inserts. After 3-day culturing, the inserts were inverted back for further endothelial cells seeding. The difference between the two co-culture systems was that a sheet of aECM was coated onto the insert membrane prior to endothelial cells seeding for the CO+aECM sample

In the beginning of the assays, 200 μl of the stock concentration of compound solution was added to the upper chamber of the insert. The lower chamber of the insert was supplemented with 1,220 μl of phenol red-free pure DMEM. The media levels inside and outside of the insert were thus level to avoid a hydraulic force influence. The sample plate was incubated at normal conditions with 5% CO_2 and at 37 $^\circ\text{C}$ except during sample extraction. At predetermined times (15, 30, 45, 60, 90, and 120 min); 110 μl of sample was withdrawn from the lower chamber while 21 μl of compensation volume of the solution was removed from the upper chamber to maintain the media volume balanced between two chambers. Optical absorbance of each sample was determined by UV absorbance using the spectrophotometer. Experiments were repeated three times for each test compound on different samples, respectively. Concentration values ($\mu\text{g}/\text{ml}$) were calculated based on calibration curves which were experimentally obtained based on three sets of independent tests for each compound. Mass transport profiles and effective permeability coefficients were calculated subsequently. The effective permeability coefficients of different test compounds across different sample setups were calculated using the following equation and the results are summarized in Table 1 [28]:

$$P_e = \frac{V}{A} \left[\frac{M_R/M_D}{t} \right]$$

Where V is the volume of the donor solution in the upper chamber, A is the surface area of the insert membrane, M_R is the mass of the test compound in the lower chamber (mol), M_D is the mass of the donor compound in the upper chamber (mol), and t is the time (s). Even though compensation volume of liquid was removed each time from both chambers to maintain the liquid level, the mass was calculated based on the initial volume because concentration was the value to be recorded, which would not be affected by the changing of the volume.

Morphology and Electron Microscopy

The morphology of endothelial cells and astrocytes in culture has been examined by an inverted microscope at the magnification of $\times 200$. A hand-held digital single lens reflex camera (Pentax K100D at 35-mm focal length with aperture of 1:4) was used to take images directly from the eye-piece of the inverted microscope.

Intracellular tight junctions were examined by scanning electron microscopy (SEM). At the end of the culturing period samples were prepared for SEM examination. Briefly, samples were fixed with 10% glutaraldehyde overnight; the fixed samples were serially dried by 10%, 30%, 50%, 75%, 90%, and 100% ethanol. After the last drying, the samples

Table 1 Effective permeability coefficients of test compound across different sample setups.

P_e ($\times 10^{-6}$ cmsec $^{-1}$)	Calcein (MW=622.55)	Caffeine (MW=80.70)	DOX (MW=579.98)
“EC” samples	2.90 \pm 0.55	11.07 \pm 3.02	4.87 \pm 1.18
“CO” samples	2.05 \pm 0.48	8.33 \pm 1.45	2.66 \pm 0.80
“CO+aECM” samples	1.33 \pm 0.25	8.14 \pm 1.61	2.38 \pm 0.73
Blank controls	7.10 \pm 0.35	14.44 \pm 0.68	8.61 \pm 0.46

were treated with hexamethyldisilazane for 3 min. Then, these samples were mounted onto conductive carbon tabs and freeze-dried overnight. Samples were examined by JEOL 6335 scanning electron microscope (SEM).

Western Blot Analysis

Western blot analysis was employed to determine the expression of occludin. For selected samples setups including “EC”, “CO”, and “CO+aECM”, at the end of the culture period, cells were collected from both sides of the inserts and solubilized with lysis buffer (5 mM EDTA, 10 mM Tris buffer, 125 mM NaCl, 1% Triton X-100, and protease inhibitor cocktail, Thermo Scientific). The cell lysate was subjected to 10% SDS-PAGE resolving gel and transferred onto a nitrocellulose membrane. The nitrocellulose membrane was blocked with 5% BSA for 1 h, and then incubated with primary antibody (rabbit anti-occludin, US Biological) overnight at 4 °C, followed by incubation with horse radish peroxidase-conjugated anti-rabbit IgG as secondary antibody (US Biological) for another hour. The immunoreactive bands were detected by a chemiluminescent kit (LumiGLO, Cell Signaling Technology, Inc) on Pierce CL-Xposure films (Fisher Scientific). Positive control occludin recombinant protein was purchased from Novus Biologicals (Littleton, CO).

Immuno-Fluorescence

The expression of occludin was further verified by immuno-fluorescence assay. At the end of the culturing period, selected setups including “EC”, “CO”, and “CO+aECM” were treated immediately with ice-cold 0.2% Triton X-100 for 2 min. Then, the cells were fixed directly on the culture inserts by 3% paraformaldehyde in PBS for 30 min at room temperature. After fixation, the samples were treated with ice-cold 0.05% Triton X-100 in PBS for 5 min. Then, the samples were blocked by 5% BSA in room temperature for 1 h. After blocking, the samples were incubated with 1:20 (5 µg/ml) rabbit anti-occludin primary antibody in room temperature for 1 h. And finally the samples were incubated with FITC-conjugated goat anti-rabbit IgG in room temperature for 30 min. The samples were examined by IX81 fluorescent microscope.

SRB Assay

The amount of astrocytes that fell from the basal sides of the insert membranes from the co-culture samples were evaluated by *in vitro* colorimetric SRB assay. This assay determines cell density based on the measurement of cellular protein content in the living cell that binds to the specific SRB dye [29]. At the end of culturing period, the well bottoms of the “CO” and “CO+aECM” samples on the 24-well plates were fixed for 30 min by 50% TCA. The fixed wells were rinsed four times with tap water and air dried before SRB staining. It took 30 min for 0.1% SRB diluted in 1% acetic acid to stain the dried well bottoms where the astrocytes fell. The stained samples were rinsed with 1% acetic acid to remove unbound dye and dried over night until no standing moisture was visible. Finally, the stained wells were solubilized by 10 mM Trizma base solution and optical absorbance was measured at 520 nm by a GNEios TECAN micro plate reader (Phoenix Research, Candler, NC). The 24-well plates were shaken for 5 min before measurement to facilitate the extraction, solubilization, and mixing of SRB dye molecules. Cell number calibration curve was generated on the same brand 24-well plate bottoms. In order to reduce possible background noise generated from the plastic wells, the optical absorbencies were taken each time for the

blank wells and the values were subtracted from the readings to get the normalized final values. The final experimental results were expressed as the number of cells calculated based on the linear relationship between the optical absorbance and cell numbers.

Statistical Analysis

Minimum of three independent experiments were performed to be presented in the final quantitative results. Results are expressed as mean value \pm standard deviation. Proper statistical analyses were performed in Microsoft Excel 2003 for corresponding data sets.

Results

Cell Morphologies

Both astrocytes and endothelial cells started to attach and spread in the culture vessel bottom within 12 h of plating. Figure 2 shows the morphologies of astrocytes and endothelial cells growing on tissue 24-well culture plates and COL Transwell inserts, respectively. Astrocytes' star-like shape was obvious from Fig. 2a. The author also noticed the astrocytes grew faster than the endothelial cells and were more easily aggregated. Figure 2b shows endothelial cells spreading on the plastic flask bottom. The typical endothelial squamous shapes were also easy to distinguish from the picture. Endothelial cells attached well on the collagen-coated filter surface of COL Transwell inserts. The structure of the collagen-coated fibrous PTFE insert membrane could be identified under the microscope in Fig. 2c. There was no obvious morphological difference between the endothelial cells growing on normal culture vessel and endothelial cells growing on the COL Transwell inserts.

Figure 3 shows an example of an automatically delaminated confluent astrocyte layer. Such a confluent layer was a homogeneous sheet full of astrocyte cell bodies providing an ideal scaffolding substrate when decellularized for endothelial cells seeding. After being decellularized by the lysis solution, the cell layer looked different from normal confluent astrocytes sheet under electron microscope (SEM). Figure 4 compares the distinguished

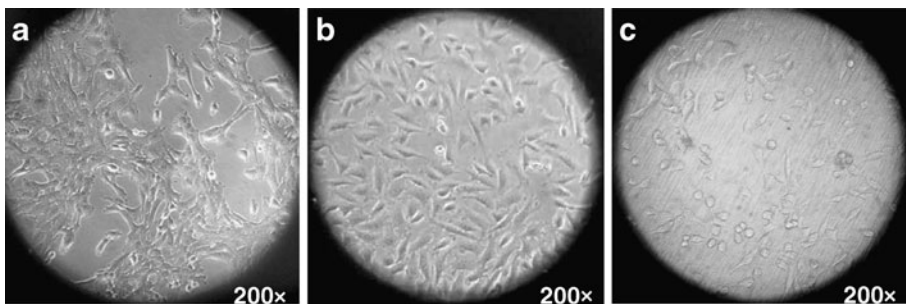
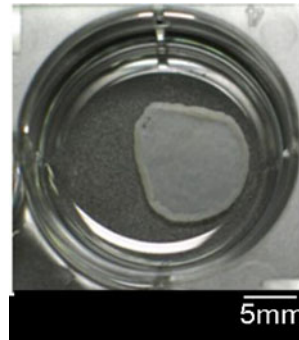


Fig. 2 Cell morphologies from the inverted microscope. **a** Astrocytes on T-75 flask bottom at $\times 200$ magnification. **b** ECs on T-75 flask bottom at $\times 200$ magnification. **c** ECs on COL-insert at $\times 200$ magnification

Fig. 3 Confluent astrocyte sheet delaminated from the culture plate well bottom forming a sticky yet elastic layer



SEM images at $\times 2000$ magnification for normal and the decellularized astrocytes layer, respectively. The normal astrocytes appeared to be rounder and microvilli were visible. More hollow spaces were observed for the decellularized astrocyte sheet which is ideal to structurally serve as aECM for endothelial cells seeding.

Fig. 4 SEM images at $\times 2000$ magnification. **a** Confluent AS layer after 10-day culture period. **b** aECM decellularized from a confluent AS layer from the same condition as shown in A

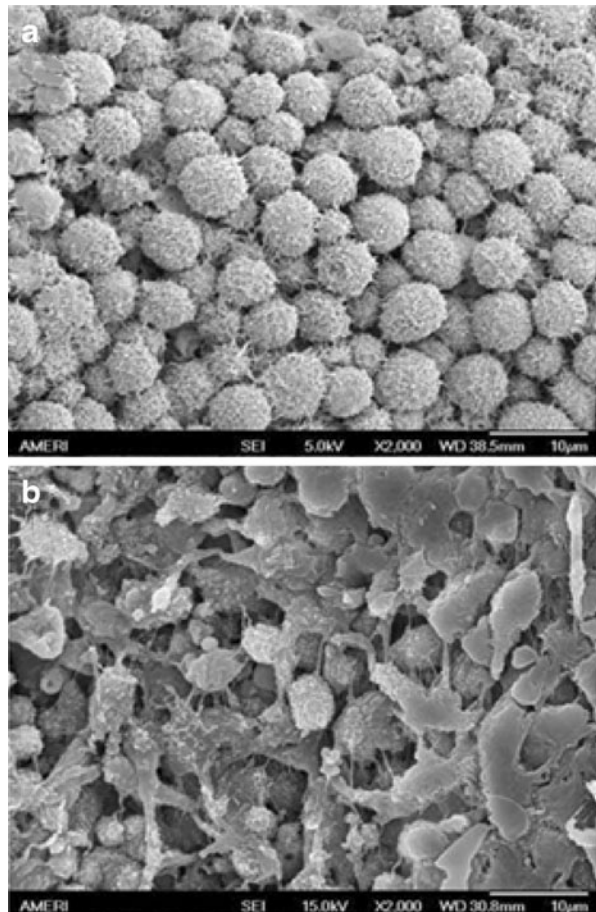
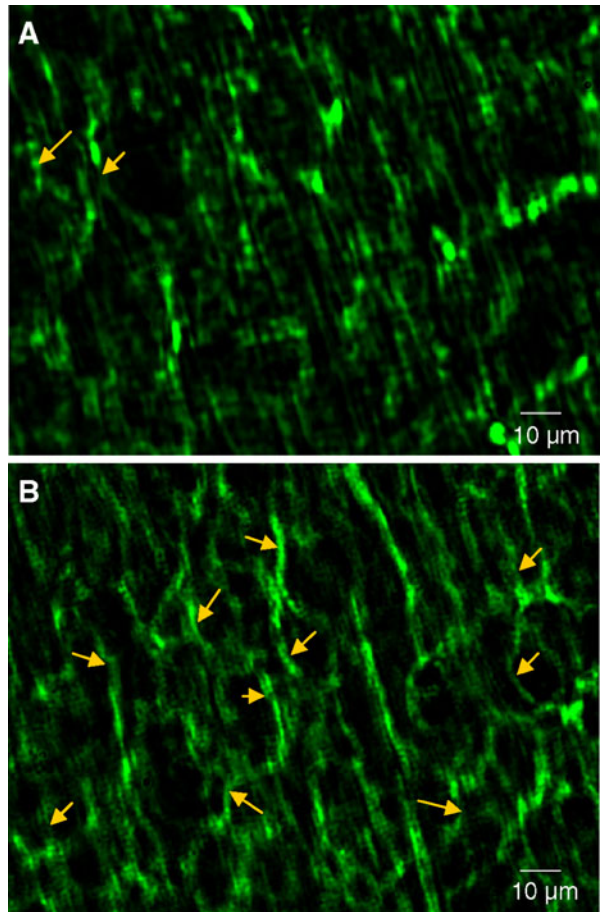


Fig. 5 Immuno-staining of occludin on the co-cultured BBB in vitro model samples. Both samples were cultured for 9 days after ECs were seeded. The silhouettes are visible at the magnification of $\times 600$, cells' edges are selectively marked by arrows. **a** CO sample. **b** CO+aECM sample



Immuno-Detection of Tight Junction Protein Occludin

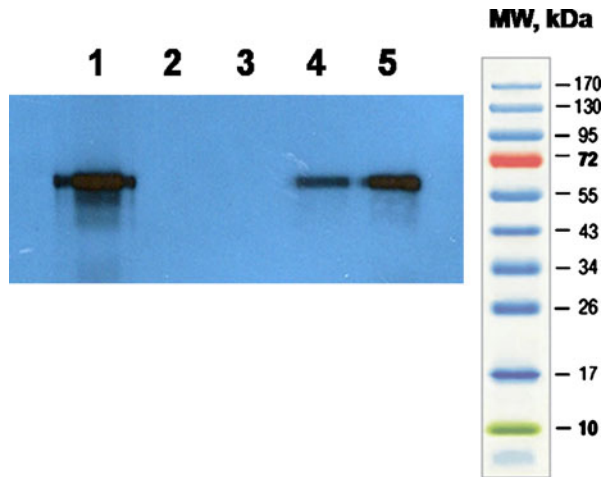
Immuno-Fluorescence Microscopy

The immuno-stained occludin contours for both “CO” and “CO+aECM” samples are shown in Fig. 5. The fluorescence image of the “EC” sample was completely dark so it was not shown here. Tight junction protein occludin's contours could be observed from both co-cultured sample setups. However, the cells contours marked by the stained occludin were more obvious on the “CO+aECM” samples than those on the “CO” samples. There was a blurred pattern of green color in Fig. 5a which could be the noise coming from the PTFE fibers from below the cell layer but not the stained protein itself. The cell silhouettes on Fig. 5b were much easier to distinguish than those on Fig. 5a because of the higher density of the stained occludin on the “CO+aECM” samples.

Western Blot Analysis

Expression of occludin was further detected by Western blot assay. Figure 6 shows the Western blot analysis results of different samples compared with positive control. Results

Fig. 6 Western blot analysis result of occludin in different sample setups including EC sample (*lane 2*), CO sample (*lane 4*), and CO+aECM sample (*lane 5*). The expression bands were compared with the positive control expressed at the molecular weight at around 60 kDa



revealed the presence of occludin specific band at around 60 kDa. The “CO+aECM” sample demonstrated higher level of occludin expression as compared to the “CO” sample. The “EC” sample didn't show any specific band, or the expression level was not high enough for detection under the same experimental conditions.

TEER Measurements

A total of 13 trials have been performed for this study. Earlier attempts included several other sample setups which were determined to be unsuccessful. The data from trials #7 through #13 will be reported here for discussion. Figure 7 collectively shows the TEER values of trials #7 through #10 for the samples that were cultured for 9 days after the endothelial cells were seeded. All the samples showed trends of TEER value increments especially in the beginning few days. For all the three different sample setups, the highest TEER values were observed at around day 7. TEER values were found to decline starting from day 8, possibly due to deterioration of the cell layers, where astrocytes and endothelial cell layers started to delaminate due to full confluency. Thus, trials # 11 through #13 were cultured for 7 days to be used in the transport study. The TEER values for trials #11 through #13 are collectively shown in Fig. 8.

Both Figs. 7 and 8 show that “CO+aECM” had the highest TEER values among the three setups, where the highest value was around $350 \Omega\text{cm}^2$, while the “EC” samples showed the lowest TEER values. One-way analyses of variance (ANOVA) analysis showed that “EC”, “CO”, and “CO+aECM” samples were significantly different from each other on a daily basis: the TEER values for both “CO” and “CO+aECM” samples were significantly higher than the “EC” samples for all the trials by one-way ANOVA analysis when $\alpha=0.05$ ($p=2.06 \times 10^{-12}$ on day 7). The TEER values for “CO+aECM” samples were also significantly higher than the “CO” samples by one-way ANOVA analysis when $\alpha=0.05$ ($p=3.78 \times 10^{-5}$ on day 7). The p value for the significance between “CO” and “EC” samples was 3.31×10^{-8} on day 7. However, since there were no literature “CO+aECM” TEER value data to compare with our own “CO+aECM” data, additional studies including transport study and immuno-chemistry studies are needed to further evaluate the endothelial tight junction in all the samples.

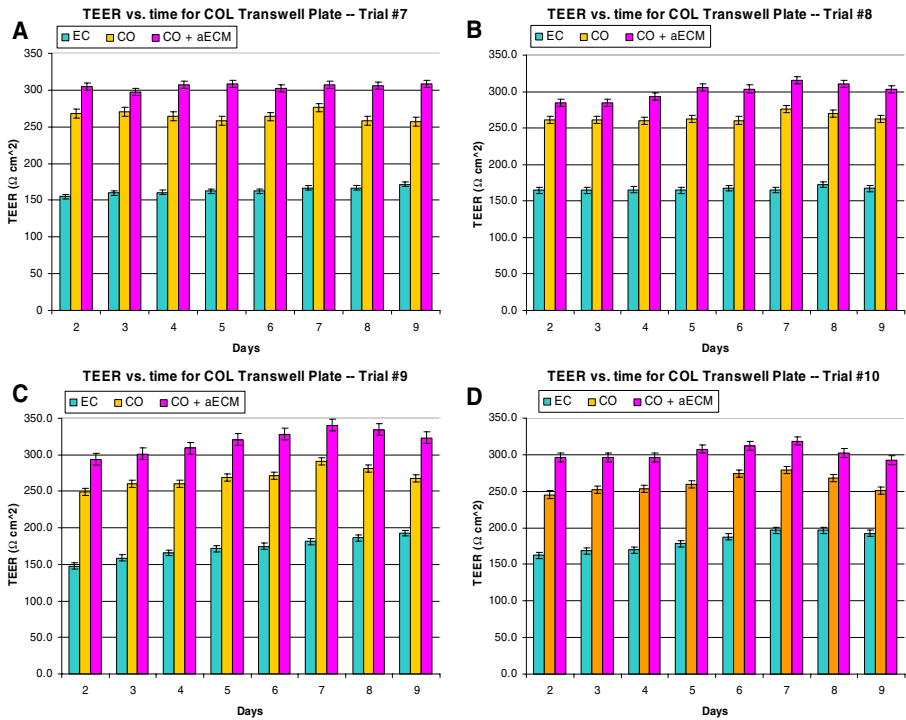


Fig. 7 TEER values of EC, CO, and CO+aECM samples from trials #7 through #10

Transport Studies

The integrity of different sample setups was assessed by studying the transport of several compound solutions with different properties across the sample membranes. Mass transport profiles of different compounds across different sample setups are summarized in Fig. 9.

Transport of Calcein Solution Across Different Sample Setups

Calcein (molecular weight (MW)=622.53) has UV absorption peak at around 490 nm and was used as a reference indicator in our experiments to evaluate the compound transport across different sample membranes [30]. All the samples with cells prevented more calcein transport over time across the membrane comparing to the blank insert membranes. Both of the co-cultured samples demonstrated greater ability to prevent calcein from permeating across the membranes over time compared with ECs only sample. The “CO+aECM” samples prevented most calcein from diffusing across the sample membrane. One-way ANOVA analysis showed that all the three samples setups were significantly different from each other over time (when $\alpha=0.05$, $P_{15 \text{ min}}=1.66 \times 10^{-6}$, $P_{30 \text{ min}}=2.42 \times 10^{-9}$, $P_{45 \text{ min}}=1.71 \times 10^{-9}$, $P_{60 \text{ min}}=3.67 \times 10^{-9}$, $P_{90 \text{ min}}=1.01 \times 10^{-8}$, $P_{120 \text{ min}}=2.25 \times 10^{-8}$). All the samples were significantly different from the blank control over time (when $\alpha=0.05$, $P_{15 \text{ min}}=4.58 \times 10^{-10}$, $P_{30 \text{ min}}=2.66 \times 10^{-5}$, $P_{45 \text{ min}}=1.65 \times 10^{-5}$, $P_{60 \text{ min}}=1.08 \times 10^{-5}$, $P_{90 \text{ min}}=4.78 \times 10^{-6}$, $P_{120 \text{ min}}=3.34 \times 10^{-6}$).

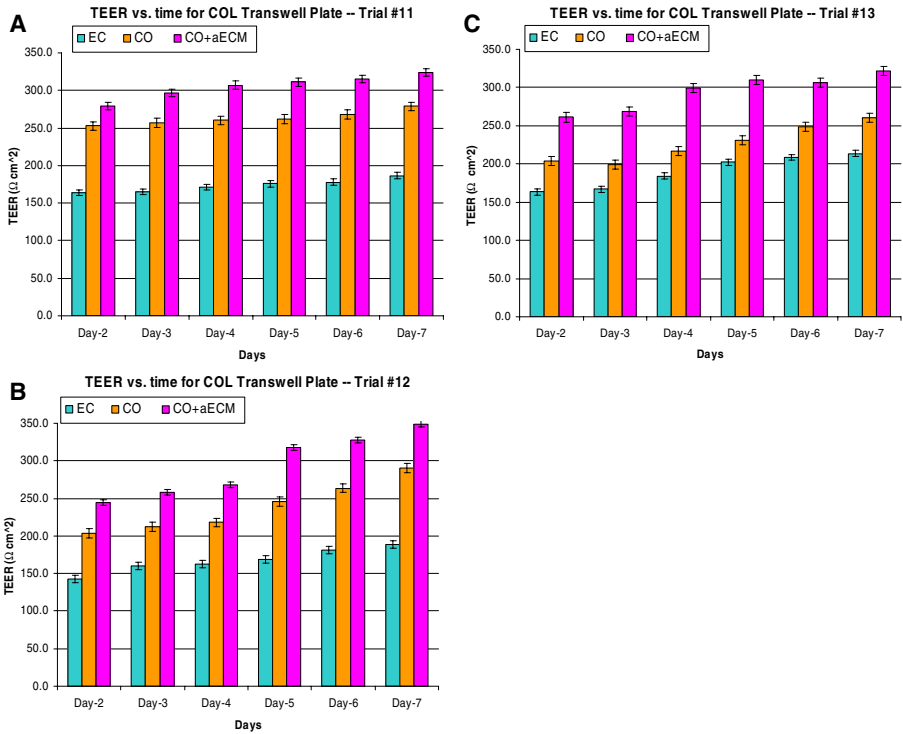


Fig. 8 TEER values of EC, CO, and CO+aECM samples from trials #11 through #13

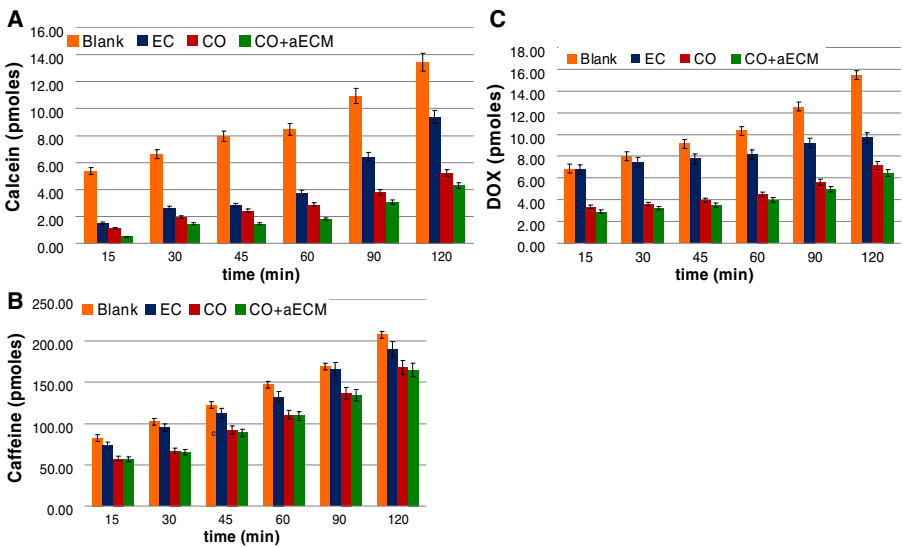


Fig. 9 Mass transport profiles of calcein (a), caffeine (b), and DOX (c) across blank insert filter (for calcein), EC, CO, and CO+aECM samples respectively

Transport of Caffeine Solution Across Different Sample Setups

Caffeine (MW=80.7, UV absorbance peak at around 275 nm) is a small molecule and is known to be distributed from plasma into the brain and CNS [31, 32]. Over time, more and more caffeine permeated across the membrane. One-way ANOVA analysis showed that there was no significant difference between the “EC” samples and the blank controls (when $\alpha=0.05$, $P_{15 \text{ min}}=0.0499$, $P_{30 \text{ min}}=0.1612$, $P_{45 \text{ min}}=0.1118$, $P_{60 \text{ min}}=0.0649$, $P_{90 \text{ min}}=0.7130$, $P_{120 \text{ min}}=0.0918$). Also, no significant difference was found between the “CO” & “CO+aECM” samples controls (when $\alpha=0.05$, $P_{15 \text{ min}}=0.6927$, $P_{30 \text{ min}}=0.5030$, $P_{45 \text{ min}}=0.3997$, $P_{60 \text{ min}}=0.7548$, $P_{90 \text{ min}}=0.6773$, $P_{120 \text{ min}}=0.6849$). However, the co-culture samples were significantly different than the “EC” samples (when $\alpha=0.05$, $P_{15 \text{ min}}=0.0009$, $P_{30 \text{ min}}=0.0001$, $P_{45 \text{ min}}=0.0019$, $P_{60 \text{ min}}=0.0049$, $P_{90 \text{ min}}=0.0032$, $P_{120 \text{ min}}=0.0254$) or the blanks (when $\alpha=0.05$, $P_{15 \text{ min}}=3.07 \times 10^{-5}$, $P_{30 \text{ min}}=6.93 \times 10^{-6}$, $P_{45 \text{ min}}=0.0001$, $P_{60 \text{ min}}=0.0002$, $P_{90 \text{ min}}=0.0007$, $P_{120 \text{ min}}=0.0014$).

Transport of Doxorubicin Solution Across Different Sample Setups

Doxorubicin (DOX, MW=543.52) is a chemotherapy agent and a known substrate of p-glycoprotein on the BBB [33]. In our experiment, DOX was used as one of the drug candidates to test the transport across the in vitro model sample membranes. One-way ANOVA analysis revealed that all the three samples setups were significantly different from each other (when $\alpha=0.05$, $P_{15 \text{ min}}=1.95 \times 10^{-6}$, $P_{30 \text{ min}}=2.08 \times 10^{-6}$, $P_{45 \text{ min}}=2.72 \times 10^{-6}$, $P_{60 \text{ min}}=4.65 \times 10^{-6}$, $P_{90 \text{ min}}=1.35 \times 10^{-5}$, $P_{120 \text{ min}}=0.0002$). All of the samples were also significantly different from the blank control (when $\alpha=0.05$, $P_{15 \text{ min}}=9.24 \times 10^{-8}$, $P_{30 \text{ min}}=7.62 \times 10^{-8}$, $P_{45 \text{ min}}=6.02 \times 10^{-8}$, $P_{60 \text{ min}}=6.29 \times 10^{-8}$, $P_{90 \text{ min}}=8.75 \times 10^{-8}$, $P_{120 \text{ min}}=1.05 \times 10^{-7}$). Four out of six of the “CO+aECM” samples prevented significantly more DOX from permeating through the membrane than the “CO” samples (when $\alpha=0.05$, $P_{15 \text{ min}}=0.0245$, $P_{30 \text{ min}}=0.0616$, $P_{45 \text{ min}}=0.0444$, $P_{60 \text{ min}}=0.0422$, $P_{90 \text{ min}}=0.0456$, $P_{120 \text{ min}}=0.0657$).

Basal Sides Cell Loss Analysis

SRB optical absorbencies from the well bottoms of four trials were obtained, with four replications of each trial, respectively. The normalized optical absorbance values were calculated using the equation obtained from the calibration curve, and the results are displayed in Table 2 in terms of cell numbers. Cell loss from the two setups were shown to be statistically significant by *t* test analysis when $\alpha=0.05$ ($p=1.98 \times 10^{-7}$).

Table 2 Average number of astrocytes fell onto well bottoms from 4 trials.

	Average astrocytes loss (cells)	Standard deviation (cells)
CO samples	77,928	1,803
CO+aECM Samples	40,269	2,662

Discussion

Primary Cells Versus Immortalized Cell Lines

Even though primary cells are still one of the most popular choices in *in vitro* studies, it is not a simple or cost efficient approach to obtain the cells. In an example of obtaining rat brain endothelial primary cells described by Diglio et al., with an appropriately euthanized rat, various steps had to be performed which included surgically removal of brain hemispheres from the skull, removal of unwanted blood vessels and meninges, mincing the brain tissue, followed by 3 h of digestive incubation containing 0.5% Dispase [34]. The tissue mixture then had to go through a series centrifugation in different medium such as 15% Dextran, growth medium, followed by another 14–16 h of incubation in growth medium containing 5% serum and 1 mg/ml collagenase/dispase to further remove basement membranes and pericytes. The obtained mixture would undergo repeated centrifugation and rinsing procedures all in 5% serum supplemented growth medium. The obtained pellet was subject to centrifugation in 50% Percoll gradient solution to remove cellular debris and red blood cells. The final pellet was centrifuged again in 10% serum supplemented growth medium to further remove impurities before seeding. According to the protocol, 2–4 g surgically obtained brain tissue can yield approximately $0.4\text{--}0.7 \times 10^6$ cells. The obtained cells can be seeded at the density of $0.5 \times 10^6/\text{cm}^2$ on a previously prepared collagen coated flask which was kept at 4 °C.

Even though primary cell cultures seem to have higher *in vitro*–*in vivo* correlations, the drawbacks are also quite obvious. The aforementioned cell obtaining process is time and effort consuming: it requires at least two full days to perform all the procedures with various chemicals and solutions for different purposes. The obtained cells have no assurance to be reliable. Contamination and foreign objects can be easily introduced in the many various steps. The cell quality relies practically on the proficiency of the operator, and the outcomes can be subjective and differ from batch to batch, person to person. Variations and inconsistency are inevitable. The authors used to try to implement primary culture in the very early stage of the study but were discouraged but the tedious and ultimately non fruitful practice.

The source of the primary cells can be limiting due to the availability and high price of the animals too, let alone meeting the requirement of a desirable large quantity. Unfortunately, primary cell cultures can be only maintained for very limited passages before losing their characteristics, when apoptosis, and altered cytokine susceptibility occurs [22, 25, 35]. This means multiple animals have to be sacrificed when more and new cells are needed, and the growing demand of primary cells has already created ethical problems for scientist using animals [35].

On the other hand, immortalized cell lines have their unique attractive advantages. Same as primary cells, immortalized cells are initially obtained from isolating desired cells from animal sources. However, these obtained cells will undergo an altering process where, most usually through viral transformation, the lengths of the telomeres on the cells are maintained so that replicative senescence is avoided [25]. Thus, immortalized cell lines can usually be cultured for at least more than 25 passages before any cell crisis, enabling large scale experimental design.

The immortalization procedure is a fairly simply procedure, and best of all, this procedure will usually be accomplished by the cell vendors but not the researchers. Nowadays, more and more immortalized cell lines are available from reliable commercial sources at relatively low costs, especially when compared to all the work and effort that

have to be put into primary cell culture and maintenance. For example, in this particular study, the authors purchased both cell lines from ATCC with the total price of under \$500. Upon receiving, the cells were cultured in appropriate ways to expand the numbers and most of them were later cryo-preserved for future use. The cells used in our assessment were from passage 2 to passage 10. No significant difference was observed between samples made from different passages of the cells, thus the consistency of the in vitro samples was made possible. If the authors chose to use primary cells, for each type of the cell, 2 to 3 days would have to be dedicated to cell isolation. The cost for all the various chemicals may add up to several hundred dollars. Rat would be a favorable choice of animal since they are relatively easier to obtain and less costly, but each rat can still cost from \$20 to nearly \$100, let alone the special trained personnel needed to handle the animal. Even if the primary cells were successfully isolated and expanded, other animals will have to be sacrificed before the passage number reaches ten. There could be variance between each passage, and also between animals. The efficiency difference between primary cells and immortalized cell lines is apparent. To the author's best knowledge, no group has reported successful results from in vitro BBB models with aECM using commercially available immortalized cell lines. The study conducted in this paper could be an example of in vitro BBB modeling using immortalized cell lines.

The Contributions of the aECM

TEER value is an important evaluation method to check the integrity of in vitro tight junction formation. In our assessment, the “CO+aECM” sample demonstrated significantly higher TEER values among all the test samples, while the “EC” samples showed the lowest values. On day 7, the average TEER values for “CO” and “CO+aECM” samples were $281.01 \Omega\text{cm}^2$ and $325.21 \Omega\text{cm}^2$, respectively. The TEER values were significantly higher than the ECV304 cell line ($100 \Omega\text{cm}^2$), which has been used for feasible immortalized BBB models by several groups, and found to have relative high correlation with in vivo and in vitro permeability studies [36, 37]. As in vitro models, the TEER values of our samples were not expected to be as high as those found in in vivo environment, or even to be as high as some primary cell cultures such as the primary bovine brain endothelial cell culture carried out by Garberg et al. where TEER value had been found to be 500–800 Ωcm^2 [21]. The overall average TEER values of the “CO+aECM” samples fell in between the primary culture and the relatively successful immortalized BBB models. The author is confident that the “CO+aECM” can serve as a relevant BBB in vitro model for further assessments.

Since no group has reported solute transport for the selected test compounds in similar setups, the comparison of the mass transport profiles between different sample setups is more of our investigation focus. Since calcein hasn't found to be reactive with the BBB, and its molecular weight is around the threshold, it was employed in our transport assessment because of its excellent linear optical absorbance calibration curves. The amounts of calcein transported across the samples membranes were used as an indicator for molecules of its size. Statistical analysis showed that all the sample setups were different between each other, and the “CO+aECM” samples prevented the most amount of calcein transport with the effective permeability coefficient equaled to $(1.33 \pm 0.25) \times 10^{-6} \text{ cmsec}^{-1}$. As a small molecule with its molecular weight well below the threshold, the amounts of caffeine transported across the membranes were much more than those of calcein. However, there was no significant difference found between the “EC” samples and the “Blank” samples, or between the “CO” samples and the “CO+aECM” samples. Even though caffeine-solute transport through the “CO” or “CO+aECM” samples was statistically significantly lower

than that of the “EC” or “Blank” samples, the p values were not as low as those in comparison in the calcein transport profiles. The effective permeability coefficients for caffeine in the different setups were almost four times of those of calcein's. These results were not surprising because caffeine was reported to be actively transported across BBB by saturable mediated processes and the results verified the theory by the high efficient permeability coefficient [31, 32]. Our assessment here served as an example of the caffeine-solute transport across the BBB. For the DOX, the transport profiles of both the “CO” and the “CO+aECM” samples were statistically significantly lower than that of the “EC” samples. And the majority of the “CO+aECM” samples prevented significantly more DOX from being transported across the sample membranes than those of the “CO” samples. The next step for the authors would be to evaluate the existence of p-glycoproteins on the sample membranes, but for now the available results could be concluded as a phenomenal proof of the existence of some DOX-resistant component on the co-culture sample membranes, which were found to be more on the “CO+aECM” samples than those on the “CO” samples.

The Western blot result indicated more occludin was expressed on the “CO+aECM” sample than on the “CO” sample, while there was no detectable occludin on the EC sample. Similar result was demonstrated by the immuno-fluorescence microscopy images where the occludin on “CO” and “CO+aECM” samples were stained and visible on the cell silhouette. These results proved that astrocytes in both co-culture samples helped induce the endothelial cells to express the tight junction protein occludin. The aECM in the “CO+aECM” sample was essential for the endothelial cells to express more occludin hence forming better tight junctions as shown in Fig. 5. The occludin expression was found to be comparable to literature as described by Garcia-Garcia et al. and Hurst et al. [2, 28].

As one of the minor study of co-culture model characteristics, the SRB staining study was performed to check the number of astrocytes that fell onto the well bottoms during the whole culture period. For both co-cultured samples, since the astrocytes were growing on the basal sides of the inserts, the cells would inevitably fall onto the wells because of gravity. However, statistical study on the SRB assay revealed that the CO+aECM samples had significantly less astrocytes loss from the basal sides of the inserts than that from the CO samples. The astrocytes loss results maybe due to the fact that astrocyte itself is involved with secretion of cellular adhesion molecules, a component of the extracellular matrix. With the existence of aECM, the co-culture present a better mimic of the real BBB and the extracellular components from the aECM helped the astrocytes on the basal side “stick” tighter to fight the pull from gravity. The integrity of the BBB is also revealed in part by this study.

The addition of one extra layer of aECM may be argued to be the reason of higher TEER values and lower mass transport. However it is important to notice the higher tight junction protein occludin expression qualitatively demonstrated by both Western blot and immuno-fluorescence microscopy. It was also interesting to discover that CO+aECM samples had less cell loss on the basal sides of the inserts comparing to CO samples at the end of the experiments. This phenomenon may indicate the important role astrocytes played in extracellular matrix secretion as well as the interaction between astrocytes and endothelial cells. In the meanwhile, it was experimentally observed that the aECM gradually became less visible during the culture period. This phenomenon can be explained by the extra cellular components secreted by the astrocytes which were gradually consumed by the co-culture system and thus the “extra” layer of aECM was diminishing over time. However, the trends of the quantitative results (TEER and transport) didn't change over time with the disappearing of the aECM. This suggested that the aECM were a better mimic of the blood-

brain barrier basement membrane and helped the ECs to maintain the tight junction features. Astrocyte derived aECM thus proved its important role in providing a suitable basement membrane environment for the tight junction formation in every aspect.

Conclusion

The main focus of this specific study can be broken down into two independent but related facets: to investigate the feasibility of using commercially available immortalized cell lines as an effective alternative of primary cell cultures in BBB in vitro modeling; and to explore the effect of astrocyte derived aECM as an endothelial cell seeding scaffold on in vitro BBB co-culture models.

All the sample setups in our study were performed and reproduced in uniform manner under the same experiment conditions. Quantitative and qualitative experiments including TEER measurements, transport studies, Western blot analysis, Immuno-fluorescence microscopy, SEM analysis, and the SRB assay collectively suggested that the CO+aECM sample served as a feasible in vitro BBB model, with superior test results than the CO and EC samples. In the CO+aECM sample, the aECM provided a biomimick of a basement membrane that is similar to the actual brain microvasculature environment for the endothelial cells. The novel co-cultured BBB in vitro model with aECM also proved to be reproducible, reliable, and easy to manage by using commercially available immortalized cell lines. Our model provides a convenient and cost effective alternative platform for in vitro drug testing and development.

Acknowledgements This current work is partially supported by 2008 FIU Faculty Research Award to Dr. Chen-Zhong Li and the Dissertation Year Fellowship to Zhiqi Zhang granted by the Graduate School of Florida International University. Special thanks to Dr.Wang, Xiaotang's Biochemistry Lab and his Ph.D. student Wang, Zheng and Hui Tian for their kind help on the Western blot assay.

References

1. Zhang, Y., & Miller, D. W. (2005). Drug Delivery Principles and Applications. In B. Wang, T. Siahhan, & R. A. Soltero (Eds.), *Hoboken*. New Jersey: John Wiley & Sons, Inc.
2. Garcia-Garcia, E., Gil, S., Andrieux, K., Desmaele, D., Nicolas, V., Taran, F., et al. (2005). *Cellular and Molecular Life Sciences*, 62(12), 1400–1408.
3. Engelhardt, B. (2003). *Cell and Tissue Research*, 314(1), 119–129.
4. Hawkins, B. T., & Davis, T. P. (2005). *Revelation*, 57(2), 173–185.
5. Zlokovic, B. V. (2008). *Neuron*, 57(2), 178–201.
6. Pardridge, W. M. (1999). *Journal of Neurovirology*, 5(6), 556–569.
7. Rubin, L. L., & Staddon, J. M. (1999). *Annual Review of Neuroscience*, 22(1), 11–28.
8. Haseloff, R. F., Blasig, I. E., Bauer, H. C., & Bauer, H. (2008). *BBA-Biomembranes.*, 1778(3), 588–600.
9. Kacem, K., Lacombe, P., Seylaz, J., & Bonvento, G. (1998). *Glia*, 23(1), 1–10.
10. Barrios-Rodiles, Brown, M. K. R., Ozdamar, B., Bose, R., Liu, Z., Donovan, R. S., et al. (2005). *Science*, 307(5715), 1621–1625.
11. Li, D., & Mrsny, R. J. (2000). *The Journal of Cell Biology*, 148(4), 791–800.
12. Yu, A. S. L., McCarthy, K. M., Francis, S. A., McCormack, J. M., Lai, J., Rogers, R. A., et al. (2005). *American Journal of Physiology. Cell Physiology*, 288(6), 1231–1241.
13. Murata, M., Kojima, T., Yamamoto, T., Go, M., Takano, K., Osanai, M., et al. (2005). *Experimental Cell Research*, 310(1), 140–151.
14. Osanai, M., Murata, M., Nishikiori, N., Chiba, H., Kojima, T., & Sawada, N. (2006). *Cancer Research*, 66(18), 9125–9133.

15. Wang, Z., Mandell, K. J., Parkos, C. A., Mrsny, R. J., & Nusrat, A. (2005). *Oncogene*, 24(27), 4412–4420.
16. Mizuguchi, H., Utoguchi, N., & Mayumi, T. (1997). *Brain Research Protocols*, 1(4), 339–343.
17. Abbott, N. J., Rönnbäck, L., & Hansson, E. (2006). *Nature Reviews. Neuroscience*, 7(1), 41–53.
18. Haring, H. P., Akamine, B. S., Habermann, R., Koziol, J. A., & Del Zoppo, G. J. (1996). *Neuropath. Exp. Neur.*, 55(2), 236–245.
19. Milner, R., & Campbell, I. L. (2002). *Molecular and Cellular Neurosciences*, 20(4), 616–626.
20. Abbott, N. J. (2004). *Drug. Discov. Today.: Technologies*, 1(4), 407–416.
21. Garberg, P., Ball, M., Borg, N., Cecchelli, R., Fenart, L., Hurst, R. D., et al. (2005). *Toxicol In Vitro*, 19(3), 299–334.
22. Yoo, J. W., Kim, Y. S., Lee, S. H., Lee, M. K., Roh, H. J., Jhun, B. H., et al. (2003). *Pharmaceutical Research*, 20(10), 1690–1696.
23. Li, C.-Z., Taniguchi, I., & Mulchandani, A. (2009). *Bioelectrochemistry*, 75, 182–188.
24. Gray, T. E., Guzman, K., Davis, C. W., Abdullah, L. H., & Nettesheim, P. (1996). *Am. J. Resp. Cell. Mol.*, 14(1), 104–112.
25. Levashova, Z. B., Plisov, S. Y., & Perantoni, A. O. (2003). *Kidney International*, 63(6), 2075–2087.
26. Li, C.-Z., Nishiyama, K., Taniguchi, I. (2000). *Electrochimica Acta*, 45, 2883–2888.
27. Radany, E. H., Brenner, M., Besnard, F., Bigornia, V., Bishop, J. M., & Deschepper, C. F. (1992). *P. Natl. Acad. Sci. USA*, 89(14), 6467–6471.
28. Hurst, R. D., & Fritz, I. B. (1996). *Journal of Cellular Physiology*, 167(1), 81–88.
29. Vichai, V., & Kirtikara, K. (2006). *Nature Protocols*, 1(2), 1112–1116.
30. Flaten, G. E., Dhanikula, A. B., Luthman, K., & Brandl, M. (2006). *European Journal of Pharmaceutical Sciences*, 27(1), 80–90.
31. McCall, A. L., Millington, W. R., & Wurtman, R. J. (1982). *Life Sciences*, 31, 2709–2715.
32. Nakazono, T., Murakami, T., Sakai, S., Higashi, Y., & Yata, N. (1992). *Chemical & Pharmaceutical Bulletin*, 40, 2510–2515.
33. Sadzuka, Y., Hatakeyama, H., Daimon, T., & Sonobe, T. (2008). *International Journal of Pharmaceutics*, 354(1–2), 63–69.
34. Diglio, C. A., Grammas, P., Giacomelli, F., & Wiener, J. (1982). *Laboratory Investigation*, 46(6), 554–563.
35. Herrmann, J., Gressner, A. M., & Weiskirchen, R. (2007). *Journal of Cellular and Molecular Medicine*, 11(4), 704–722.
36. Kuchler-Bopp, S., Delaunoy, J. P., Artault, J. C., Zaepfel, M., & Dietrich, J. B. (1999). *NeuroReport*, 10(6), 1347–1353.
37. Hurst, R. D., Heales, S. J. R., Dobbie, M. S., Barker, J. E., & Clark, J. B. (1998). *Brain Research*, 802(1–2), 232–240.